In Situ Calcium Carbonate Dissolution in the Pacific Ocean

R. A. Feely,[1] C. L. Sabine,[2] K. Lee,[3] F. J. Millero,[4] M. F. Lamb,[1] D. Greeley,[1] J. L. Bullister,[1] R. M. Key,[5] T.-H. Peng,[6] A. Kozyr,[7] T. Ono,[8] and C. S. Wong[9]

Abstract. Over the past several years researchers have been working to synthesize the WOCE/JGOFS global CO_2 survey data to better understand carbon cycling processes in the oceans. The Pacific Ocean data set has over 35,000 sample locations with at least two carbon parameters, oxygen, nutrients, CFC tracers, and hydrographic parameters. In this paper we estimate the in situ $CaCO_3$ dissolution rates in the Pacific Ocean water column. Calcium carbonate dissolution rates ranging from 0.01–1.1 μmol kg^{-1} yr^{-1} are observed in intermediate and deepwater beginning near the aragonite saturation horizon. In the North Pacific Intermediate Water between 400 and 800 m, $CaCO_3$ dissolution rates are more than 7 times faster than observed in mid- and deep water depths (average = 0.051 μmol kg^{-1} yr^{-1}). The total amount of $CaCO_3$ that is dissolved within the Pacific is determined by integrating excess alkalinity throughout the water column. The total inventory of $CaCO_3$ added by particle dissolution in the Pacific Ocean, north of 40°S, is 157 Pg C. This amounts to an average dissolution rate of approximately 0.31 Pg C yr^{-1}. This estimate is approximately 74% of the export production of $CaCO_3$ estimated for the Pacific Ocean. These estimates should be considered to be upper limits for in situ carbonate dissolution in the Pacific Ocean, since a portion of the alkalinity increase results from inputs from sediments.

1. Introduction

In recent years, concern about the long-term fate of anthropogenic CO_2 in the atmosphere and ocean has prompted oceanographers to re-examine the fundamental processes controlling the distributions of dissolved inorganic carbon (DIC) and total alkalinity (TA) in the oceans. Processes that increase the TA in the upper ocean facilitate the uptake of anthropogenic CO_2 from the atmosphere. Conversely, processes that reduce the TA serve to impede the uptake. The primary motivation for this research is to understand

[1]NOAA/Pacific Marine Environmental Laboratory, Seattle, Washington, USA.
[2]Joint Institute for the Study of Atmosphere and Ocean, University of Washington, Seattle, Washington, USA.
[3]School of Environmental Science and Engineering, Pohang University of Science and Technology, Pohang, Republic of Korea.
[4]University of Miami/RSMAS, Miami, Florida, USA.
[5]AOS Program, Princeton University, Princeton, New Jersey, USA.
[6]NOAA/Atlantic Oceanographic and Meteorological Laboratory, Miami, Florida, USA.
[7]Carbon Dioxide Information Analysis Center, Oak Ridge, Tennessee, USA.
[8]Hokkaido National Fisheries Research Institute, Kushiro, Japan.
[9]Institute of Ocean Sciences, Sidney, British Columbia, Canada.

Paper number .
0886-6236/02/$12.00

and quantify these processes in the Pacific Ocean.

Marine carbonates, including calcitic (e.g., coccoliths and forams) and aragonitic (e.g., pteropods) plankton neutralize anthropogenic CO_2 and add TA via the dissolution reaction:

$$CO_2 + CaCO_3 + H_2O \leftrightarrow 2HCO_3^- + Ca^{2+} \quad (1)$$

The increase in TA from this reaction enhances the ocean's capacity to absorb more CO_2 from the atmosphere. The primary contributors to this reaction are the carbonate shells of marine plankton that are produced in the euphotic zone. Upon death, the carbonate tests fall through the water column and are either dissolved or deposited in shallow or deep-sea sediments. As the oceans become enriched in anthropogenic CO_2, the locations and extent of dissolution will increase as a function of changes in the $CaCO_3$ saturation state. Until recently, it had been commonly thought that dissolution of pelagic calcium carbonate particles primarily occurs at great depths below the "carbonate lysocline" [*Sverdrup et al.,* 1941; *Broecker,* 1977]. However, recent analyses of the global carbonate budget and sediment trap data for the global oceans [*Milliman,* 1993; *Milliman and Droxler,* 1996; *Milliman et al.,* 1999] have indicated that perhaps as much as 60–80% of the calcium carbonate that is exported out of the surface ocean dissolves in the upper 500–1000 m, well above the carbonate lysocline. In this paper, we examine the WOCE/JGOFS global CO_2 survey data from the Pacific Ocean and provide new estimates of calcium carbonate dissolution rates in the water column based upon changes in TA.

2. The WOCE/JGOFS Data

Between 1991 and 1996, carbon measurements were made on 24 cruises in the Pacific Ocean. This research was a collaborative effort between 15 laboratories and 4 countries. Figure 1 shows the nearly 2000 station locations with carbon measurements in the Pacific. At least two carbon parameters were measured on all cruises, but the choice of which carbon system pairs were measured varied between cruises. The carbon system measurements are described in detail in *Feely et al.* [1999]. The quality of the carbon data was evaluated by *Lamb et al.* [2002]. A set of adjustments for certain cruises were recommended based on many lines of evidence including comparison of calibration techniques, results from certified reference material analyses, precision of at-sea replicate analyses, agreement between shipboard analyses and replicate shore-based analyses, comparison of deep water values at locations where two or more cruises overlapped or crossed, consistency with other hydrographic parameters, and internal consistency with multiple carbon parameter measurements. *Lamb et al.* [2002] estimated that the overall accuracy of the DIC data was $\sim$3 μmol kg^{-1}. TA, the second most common carbon parameter analyzed, had an overall accuracy of $\sim$5 μmol kg^{-1}. The TA was calculated for all cruises where it was not measured using the carbonate dissociation constants of *Mehrbach et al.* [1973] as refitted by *Dickson and Millero* [1987] and ancillary constants listed in the program of *Lewis and Wallace* [1998]. The final data set contained about 35,000 sample locations with DIC and TA values.

Figure 1

The corresponding chlorofluorocarbon (CFC) samples

were analyzed by the methods of *Bullister and Weiss* [1988] and the results were compiled and evaluated by the US WOCE CFC consortium. The Pacific synthesis of the chlorofluorocarbon data, led by J. Bullister, examined the overall quality of the data and ensured that all of the values were reported on the same concentration scale. Although no adjustments were made to the final reported CFC values, the data were carefully flagged based on examination of the entire data set.

3. Analysis Method

3.1. Anthropogenic CO_2

Our approach for estimating anthropogenic CO_2 in the Pacific Ocean is modified from the techniques described by *Gruber et al.* [1996]. *Gruber et al.* improved the earlier approaches of *Brewer* [1978] and *Chen and Millero* [1979] by developing the ΔC^* method. This method is based on the premise that the anthropogenic CO_2 concentration (C_{anth}) can be isolated from measured DIC values (C_m) by subtracting the contribution of the biological pumps (ΔC_{bio}), the DIC waters that would have been in equilibrium with a pre-industrial atmospheric CO_2 concentration of 280 ppm (C_{eq280}), and a term that corrects for the fact that surface waters are not always in equilibrium with the atmosphere (ΔC_{diseq}):

$$\begin{aligned} C_{anth} &= C_m - \Delta C_{bio} - C_{eq280} - C_{diseq} \\ &= \Delta C^* - \Delta C_{diseq}, \end{aligned} \quad (2)$$

Where:

C_{anth}	=	Anthropogenic carbon concentration
C_m	=	Measured total carbon concentration
ΔC_{bio}	=	Change in DIC as a result of biological activity (both organic and inorganic)
C_{eq280}	=	DIC of waters in equilibrium with an atmospheric CO_2 concentration of 280 μatm
ΔC_{diseq}	=	Air-sea difference in CO_2 concentration expressed in μmol kg^{-1} of DIC

The three terms to the right of the first equal sign make up ΔC^*, which can be explicitly calculated for each sample. The fact that ΔC^* is a quasi-conservative tracer helps remedy some of the mixing concerns arising from the earlier techniques [*Sabine and Feely,* 2000]. The ΔC_{diseq} term is evaluated over small isopycnal intervals using a water-mass age tracer such as CFCs [*Sabine et al.,* 2001]. The quasi-conservative tracer, ΔC^*, is defined as the difference between the measured DIC concentration, corrected for biology and the concentration these waters would have at the surface in equilibrium with a preindustrial atmosphere (i.e., $\Delta C^* = C_m - \Delta C_{bio} - C_{eq280}$). The ΔC^* calculation used here is essentially the same as that originally defined by *Gruber et al.* [1996] with two small differences: a modification of the preformed alkalinity term based on the new global survey data and the addition of a denitrification term in the biological correction [see *Sabine et al.,* 2001 for details].

3.2. Calcite and Aragonite Saturation

The calcite and aragonite saturation levels were calcu-

lated using the program developed by *Lewis and Wallace* [1998]. The in situ degree of saturation of seawater with respect to calcite and aragonite is the ion product of the concentrations of calcium and carbonate ions, at the in situ temperature, salinity and pressure, divided by the stoichiometric solubility product for those conditions:

$$\Omega = [Ca^{2+}] \cdot [CO_3^{2-}]/K'sp \quad (3)$$

Where the calcium concentration is estimated from the salinity, and the carbonate ion concentration is calculated from the TA data. The pressure effect on the solubility is estimated from the equation of *Mucci* [1983] that includes the adjustments to the constants recommended by *Millero* [1995].

3.3. $CaCO_3$ Dissolution

The TA has three primary components in the water column: 1) the preformed TA (TA°), fixed when the parcel of water was last in contact with the atmosphere; 2) the changes in TA resulting from the release of protons during the oxidation of organic matter, and 3) the TA added to the water column via $CaCO_3$ dissolution. In this study, we employed the TA° equation of *Sabine et al.* [2001] based on near surface (0–60 m) data from the same Pacific data set used here:

$$TA^\circ = 148.7 + (61.36 \cdot S) + (0.0941 \cdot PO) - (0.582 \cdot \theta) \quad (4)$$

where S is the salinity, $PO = O_2 + R_{O2/P}HPO_4^{2-}$ [after *Broecker,* 1974], and θ is the potential temperature. The value of $R_{O2/P}$ of 170 is used in this work [*Anderson and Sarmiento,* 1994].

The organic matter correction of *Chen* [1978], based on changes in nitrate, was also adapted for use in this study. The largest component of this correction is from the oxidation of organic nitrogen. However, a coefficient of 0.63 was proposed by *Kanamori and Ikegami* [1982] to include contributions from organic phosphorus and sulfur as well. Rather than attempting to determine preformed nitrate values, Chen's equation was converted to apparent oxygen utilization (AOU) using the *Anderson and Sarmiento* [1994] N/O_2 ratio of 16/170. For a given isopycnal surface, the changes due to $CaCO_3$ dissolution can be evaluated using what we term TA^*:

$$TA^* = 0.5(NTA - NTA^\circ) + 0.63(0.0941 \cdot AOU) \quad (5)$$

where $NTA = (TA \cdot 35)/S$, $NTA^\circ = (TA^\circ \cdot 35)/S$ and AOU is the apparent oxygen utilization. Although this general approach has been used successfully for a number of years [e.g., *Brewer et al.,* 1975; *Chen,* 1978; *Chen et al.,* 1982; *Chen,* 1990; *Sabine et al.,* 1995], the most common historical notation of ΔCa is somewhat misleading since this calculation does not involve calcium measurements and there are potential reactions, albeit minor, that could change this value without changing the dissolved calcium. We feel that the TA^* term, in the spirit of the other star terms found in the recent literature, is more appropriate [*Gruber et al.,* 1996].

4. Results and Interpretation

4.1. Distributions of DIC and TA in the Pacific Ocean

In the Pacific Ocean the lowest concentrations of DIC and TA are observed in surface waters. The surface concentrations (DIC range: 1975–2200 μmol kg^{-1}; TA range: 2200–2400 μmol kg^{-1}) are roughly correlated with salinity (Figures 2 and 3). DIC concentrations increase in the intermediate waters to form a large maximum (2325–2375 μmol kg^{-1}) at approximately 1800–2200 m in the North Pacific. In contrast, TA concentrations show local minima in the Antarctic Intermediate Water (AAIW) to the south and in the North Pacific Intermediate Water (NPIW) to the north. Below the North Pacific Intermediate Water, TA concentrations increase to a broad maximum at approximately 2200–4000 m (TA concentrations range from 2400–2460 μmol kg^{-1}). The general structure of the DIC and TA fields are similar to the density structure in the upper 1000 m. This similarity is an indication of the strong control that circulation plays in their distributions. The differences between the DIC and TA, particularly in shallow and intermediate waters, are caused by in situ remineralization processes. The DIC maximum is shallower than the TA maximum because DIC is more strongly influenced by the shallow remineralization of soft tissue organic carbon, whereas the TA is more strongly influenced by the dissolution of calcium carbonate particles deeper in the water column [*Chen,* 1990]. Except for the region north of 30°N, bottom waters have lower DIC and TA concentrations than the waters at mid-water depths because the deep and bottom water circulation goes from south to north with upward mixing such that the oldest waters are centered at mid-water depths (e.g., 2000–3000 m) of the North Pacific [*Stuiver et al.,* 1983].

Figures 2 and 3

The zonal DIC and TA isolines shoal from west to east along 30°N in the P2 section in the North Pacific (Figure 3). Deep ventilation near the Kuroshio Extension and the subsequent circulation in the subtropical gyre generates the zonal gradient of DIC and TA in the upper 1500 m of the water column. Both DIC and TA concentrations show the deepest ventilation near the coast and under the Kuroshio Extension west of 160°E. These results are consistent with the CFC and anthropogenic CO_2 distributions in the North Pacific that also indicate stronger ventilation processes in the western Pacific [*Warner et al.,* 1996; *Sabine et al.,* 2001].

4.2. Aragonite and Calcite Saturation Horizon Migrations

The level at which aragonite and calcite are in thermodynamic equilibrium is the saturation depth. This depth is significantly shallower for aragonite than calcite because aragonite is more soluble in seawater than calcite (Figure 4). There is a pronounced shoaling of the aragonite and calcite from south to north and from west to east because of the higher DIC concentrations in northern and eastern regions relative to the TA concentrations (Figure 5; *Feely et al.,* 1984). The general pattern of aragonite and calcite saturation is consistent with previous results [*Takahashi,* 1975; *Chen et al.,* 1988; *Feely et al.,* 1982, 1984, 1988; *Kleypas et al.,* 1999].

Figure 4

Figure 5

The anthropogenic CO_2 concentrations and the calculated aragonite and calcite saturation horizons are plotted

for both present day (dashed line) and pre-industrial levels (solid line) for the P15 and P2 sections (Figures 6a and 6b, respectively). The pre-industrial levels are calculated by subtracting the anthropogenic CO_2 values [*Sabine et al.,* in press] from the DIC values presented here. When the pre-industrial saturation horizons are compared to the present-day values, several distinct regions of upward migrations can be observed. The present-day aragonite saturation horizon ranges from approximately 200 m to 1320 m in the South Pacific with the greatest shoaling in the region from approximately 30°S to 5°S in the eastern South Pacific (Figure 4). In the North Pacific, the aragonite saturation horizon shoals to a minimum of 220 m at about 8°N, deepens to a maximum of about 580 m at 28°N, and shoals to its shallowest depth of approximately 120 m north of 50°N. An upward migration of the present-day saturation horizon relative to the pre-industrial saturation horizon south of 38°S is observed to be between 30–80 m in the South Pacific and between 30–100 m in the North Pacific north of 3°N. A similar shoaling of the aragonite and calcite saturation horizon is observed in the east-west P2 section (Figure 6b). The west to east shoaling of the aragonite and calcite saturation horizons are consistent with the shoaling of the TA concentrations shown in Figure 3. This shoaling is the result of the deep ventilation and anticyclonic circulation in the North Pacific.

Figures 6a and 6b

The calcite saturation sections in Figures 6a and 6b indicate that the saturation horizon is close to 3000 m in the South Pacific and dramatically shoals to about 700 m just north of 20°N in the North Pacific. From there, it shoals to a minimum at approximately 250 m north of 50°N. The data suggest a distinct upward migration of the saturation horizon north of 20°N from the pre-industrial period to the present ranging between 40 and 100 m. These results, indicating the shoaling of aragonite and calcite saturation horizons due to the effects of anthropogenic CO_2 ventilation in the surface and intermediate waters, imply that there may be a potential for enhanced dissolution of $CaCO_3$ particles in the undersaturated waters.

4.3. $CaCO_3$ Dissolution Rates

The WOCE/JGOFS global CO_2 survey in the Pacific Ocean was used for estimating $CaCO_3$ dissolution in the water column. Figure 7 shows a wedge-like cutout section of TA^* along 170°W, 30°N, and 150°W. Positive concentrations of TA^* are observed in the shallow waters near or slightly above the aragonite saturation horizon. Below this horizon, TA^* concentrations increase rapidly from about 10–40 μmol kg^{-1}. This gradient is primarily located in the Intermediate Waters of the North and South Pacific. For example, north of 20°N, the largest increase occurs between about 400–1100 m, where the TA^* increase is from $<$10 μmol kg^{-1} in the North Pacific to values $>$40 μmol kg^{-1} north of 40°N. In the South Pacific between 10°S and 45°S, where the aragonite and calcite saturation horizons are much deeper, the largest gradients are between 800 m to 1800 m. Farther south in the South Pacific, the TA^* increase begins at much shallower depths, consistent with the shoaling of the aragonite saturation horizon in these waters. These results suggest that the extent of $CaCO_3$ dissolution is somehow related to the degree of aragonite saturation.

Figure 7

Combining the above results with the apparent CFC-11 age data from the WOCE global survey data on isopycnal

surface allows us to calculate the $CaCO_3$ dissolution rates by plotting TA^* versus apparent CFC-11 ages (Figure 8). The slope of the line gives a value for the average $CaCO_3$ dissolution rate along the isopycnal surface. The method is limited to surface and intermediate waters where the apparent CFC ages are less than about 30–35 years due to mixing and dilution problems in the deeper waters. $CaCO_3$ dissolution rates calculated in this manner range from 0 in near-surface waters to a maximum exceeding 0.5 μmol kg^{-1} yr^{-1} in the intermediate waters (Figure 9). Lower rates are observed below the intermediate waters. The highest dissolution rates in the South Pacific were at depths between 1000 and 1800 m (σ_θ range: 27.3–27.6). In the North Pacific, the maximum dissolution rates were between 600 and 900 m (σ_θ range: 26.4–26.8).

Figure 8

Figure 9

Since the CFC-age method is limited to water mass ages less than about 30–35 years, we used the natural ^{14}C ages from samples collected on the same cruises to estimate $CaCO_3$ dissolution rates in deeper waters. The ^{14}C decay rate of ∼1% every 83 years makes this isotope a good age tracer for dissolution processes in the deep sea. For waters >1500 m the mean $CaCO_3$ dissolution rate in the Pacific Deep Water was determined to be 0.051 μmol kg^{-1} yr^{-1}, based on 853 data points. To define the spatial variability of the deep-water dissolution rates these data were subsetted by basin and examined on isopycnal surfaces in a manner similar to the shallow dissolution study. The dissolution rates were significantly lower than the shallow rates, ranging from 0.01 to 0.06 μmol kg^{-1} yr^{-1}. The highest rates were observed at a sigma-3 of 40.4 (Figure 10). In contrast to the shallow analysis, the South Pacific showed higher dissolution rates than the North Pacific. It is possible that the more corrosive waters of the North Pacific result in less carbonate particles actually reaching the deep waters. Contamination from bomb ^{14}C prevents us from carrying the analysis to depths much shallower than ∼1000 m.

Figure 10

One can get a sense of the dissolution throughout the water column from a plot of the average TA^* as a function of depth (Figure 11). The maximum signal is near 1100 m, just below the average depth of the aragonite saturation horizon and well above the old southward return flow. A second local maximum is observed near 3800 m, just below the calcite saturation depth. A third maximum is observed in the bottom-waters. This could be a benthic dissolution signal. Although the waters at all levels intersect the bottom, by far the largest area of bottom is associated with waters deeper than 4500 m.

Figure 11

5. Discussion

The in situ TA^* values and estimated dissolution rates presented here can be directly compared with other data on shallow and deep water dissolution of $CaCO_3$ particles in the Pacific. Recent estimates of excess Ca based on dissolved Ca measurements reported by *Chen* [in press] for a section along 150°W in the North Pacific give very similar values (10–40 μmol kg^{-1}) for depths between 300 and 1200 m as that shown in Figure 7 for the 170°W section based on the WOCE alkalinity measurements. Since the CFC-11 ages on isopycnal surfaces are very similar between 170°W and 150°W in the North Pacific [*Warner et al.,* 1996], the $CaCO_3$ dissolution rates would also be very similar. Additional direct comparisons of the $CaCO_3$ dissolution

rates are given in Table 1, which compares the new results from the WOCE survey with the results from earlier expeditions and methods [*Honjo et al.,* 1977, 1995; *Chen,* 1990]. In shallow waters (200–1300 m), the mean $CaCO_3$ dissolution rate from the WOCE results, 0.36 μmol kg^{-1} yr^{-1}, is within the range of estimates from the sediment flux losses (0.005–1.83 μmol kg^{-1} yr^{-1}) from the equatorial, tropical, and subpolar North Pacific. The results are somewhat lower than the global average sediment trap flux losses given in *Milliman et al.* [1999], but significantly higher than the average for waters deeper than 1500 m. For waters >1500 m the mean $CaCO_3$ dissolution rate (0.051 μmol kg^{-1} yr^{-1}) is near the middle of the range of estimates from the previous work (0.01–0.11 μmol kg^{-1} yr^{-1}) based on dissolved Ca and alkalinity data and deep water sediment trap flux losses.

The average TA* concentrations are highest at intermediate depths (Figure 11) because the dissolution rate in the shallow waters of the North Pacific is approximately 7 times faster than the deep-water dissolution rates. There are several possible mechanisms for the higher dissolution rates at the shallower depths, including: 1) dissolution of $CaCO_3$ particles in the guts of zooplankton [*Takahashi,* 1975; *Bishop et al.,* 1980, 1986; *Harris,* 1994; *Van der Wal et al.,* 1995; *Pond et al.,* 1995]; 2) dissolution of $CaCO_3$ particles in microenviroments where bacterial oxidation of organic matter can enhance the dissolution process [*Jansen and Wolf-Gladrow,* 2001], and 3) dissolution of the more soluble forms of $CaCO_3$ in shallow waters, including pteropods and high-Mg calcite [*Byrne et al.,* 1984; *Morse and Mackenzie,* 1990]. Recent modeling efforts by *Jansen and Wolf-Gladrow* [2001] for copepods grazing on coccolithophorids indicate that dissolution of calcite in copepod guts "does not account for the majority of the observed carbonate loss in the water column but may contribute a significant portion." On the other hand, the sharp increase in TA* near or below the aragonite saturation horizon in the North and South Pacific suggests that the more soluble carbonate phases may dissolve quite readily, and that the least soluble carbonates remain preserved during transit to deeper levels. This is in agreement with the earlier in vitro experiments by Byrne and colleagues [*Byrne et al.,* 1984; *Feely et al.,* 1988], showing that pteropod shells undergo significant dissolution below the saturation horizon. Consequently, there is probably more than one mechanism that contributes to the increased alkalinity at shallow water depths.

The total amount of $CaCO_3$ that has dissolved in Pacific waters can be determined by integrating TA* throughout the water column. To remove the contribution from dissolution outside of the Pacific basin then transported in with the deep and intermediate waters, all values were normalized to the average concentrations at 40–50°S. The total inventory of $CaCO_3$ dissolution in the Pacific north of 40°S is 157 Pg C. This should be considered to be an upper limit, since some of the alkalinity input may have originated from the sediments [*Chen,* in press]. If one takes an average Pacific waters residence time of 500 yrs [*Stuiver et al.,* 1983], this would give an average dissolution rate of approximately 0.31 Pg C yr^{-1}. This number is not exact since the residence time and dissolution rates vary with depth, but this at least provides a first order estimate of the overall dissolution rate. This estimate is approximately 74% of the export production of $CaCO_3$ estimated by *Lee* [2001] for the Pacific

Table 1

Ocean.

6. Conclusions

Measurements from the WOCE/JGOFS/DOE/NOAA global CO_2 survey in the Pacific Ocean indicate that water column dissolution of $CaCO_3$ in shallow waters <1500 m accounts for as much as 50% of the total water column dissolution. This is consistent with the reanalysis of the sediment trap data by *Milliman et al.* [1999]. These results imply that the re-supply of alkalinity to the surface waters via shallow water remineralization processes occur at much faster rates than in the deeper waters. The integrated effect in the Pacific is that up to approximately 0.31 Pg C yr^{-1} are remineralized in the water column. The measurable upward migration of the calcite and aragonite saturation horizons since the pre-industrial period suggest that the long-term impacts of $CaCO_3$ dissolution on the ocean's ability to neutralize anthropogenic CO_2 need to be considered in future biogeochemical models.

Acknowledgments. We wish to acknowledge all of those who contributed to the Pacific Ocean data set compiled for this project, including those responsible for the carbon measurements, the CFC measurements, and the Chief Scientists. This work was funded by NSF Grant OCE-0137144, NOAA/DOE grant GC99-220, and the Joint Institute for the Study of the Atmosphere and Ocean (JISAO) under NOAA Cooperative Agreement No. NA17RJ123, JISAO Contribution #896 and PMEL contribution #2438. We thank Dr. Lisa Dilling of the NOAA Office of Global Programs and Dr. Donald Rice of the National Science Foundation for their efforts in the coordination of this study.

References

Anderson, L. A., and J. L. Sarmiento, Redfield ratios of remineralization determined by nutrient data analysis, *Global Biogeochem. Cycles, 8*, 65–80, 1994.

Betzer, P. R., R. M. Byrne, J. G. Acker, C. S. Lewis, R. R. Jolly, and R.A. Feely, The oceanic carbonate system: A reassessment of biogenic controls, *Science, 226*, 1074–1077, 1984.

Bishop, J. K. B., R. W. Collier, D. R. Kettens, and J. M. Edmond, The chemistry biology and vertical flux of particulate matter from the upper 1500 m of the Panama basin**,** *Deep-Sea Res., 27A,* 615–640, 1980.

Bishop, J. K. B., J. C. Stepien, and P. H. Weibe, Particulate matter distributions, chemistry and fluxes in the Panama Basin: response to environmental forcing, *Prog. Oceanogr., 17,* 1–59, 1986.

Brewer, P. G., G. T. F. Wong, M. P. Bacon, and D. W. Spencer, An oceanic calcium problem? *Earth Planet. Sci. Lett., 26*, 81–87, 1975.

Brewer, P. G., Direct observation of the oceanic CO_2 increase, *Geophys. Res. Lett., 5*(12), 997–1000, 1978.

Broecker, W. S., 'NO', a conservative water-mass tracer, *Earth Planet Sci. Lett., 23,* 100–107, 1974.

Broecker, W. S., Recommendations of the working group on carbonate dissolution, Neutralization of fossil fuel CO_2 by marine calcium carbonate, in *The Fate of Fossil CO_2 in the Oceans*, edited by N. R. Anderson and A. Malahoff, pp. 207–212, Plenum Press, New York, 1977.

Bullister, J. L., and R. Fe. Weiss, Determination of CCl_3F and CCl_2F_2 in seawater and air, *Deep-Sea Res., 35*(5), 839–853, 1988.

Byrne, R. H., J. G. Acker, P. R. Betzer, R. A. Feely, and M. H. Cates, Water column dissolution of aragonite in the Pacific Ocean, *Nature, 312*, 321–326, 1984.

Chen, C.-T. A., Decomposition of calcium carbonate and organic carbon in the deep oceans, *Science, 201,* 735–736, 1978.

Chen, C.-T. A., and F. J. Millero, Gradual increase of oceanic CO_2, *Nature, 277*, 205–206, 1979.

Chen, C.-T. A., R. M. Pytkowicz, and E. J. Olson, Evaluation of the calcium problem in the South Pacific, *Geochem. J., 16,* 1–10, 1982.

Chen, C.-T. A., Distribution of dissolved calcium and alkalinity in the Wedell Sea in winter, *U.S. Antarctic Journal, 1983 review*, 136–137, 1983.

Chen, C.-T. A., R. A. Feely, and J. F. Gendron, Lysocline, calcium carbonate compensation depth, and calcareous sediments in the North Pacific, *Pac. Sci., 42*, 237–252, 1988.

Chen, C.-T. A., Rates of calcium carbonate dissolution and organic carbon decomposition in the North Pacific Ocean, *J. Oceanogr. Soc. Japan, 46*(5), 201–210, 1990.

Chen, C.-T. A., Self vs. dissolution-generated alkalinity above the chemical lysocline, *Deep-Sea Res. II,* in press, 2001.

Dickson, A. G., and F. J. Millero, A comparison of the equilibrium constants for the dissociation of carbonic acid in seawater media, *Deep-Sea Res., 34*, 1733–1743, 1987.

Edmond, J., On the dissolution of carbonate and silicate in the deep ocean, *Deep-Sea Res., 21*, 455–479, 1974.

Feely, R. A., and C.-T. A. Chen, The effect of excess CO_2 on the calculated calcite and aragonite saturation horizons in the northeast Pacific, *Geophys. Res. Lett., 9*(11), 1294–1297, 1982.

Feely, R. A., R. H. Byrne, P. R. Betzer, J. F. Gendron, and J. G. Acker, Factors influencing the degree of saturation of the surface and intermediate waters of the North Pacific Ocean with respect to aragonite, *J. Geophys. Res., 89*(C6), 10,631–10,640, 1984.

Feely, R. A., P. R. Betzer, R. H. Byrne, C.-T. A Chen, and J. F. Gendron, In situ calcium carbonate dissolution in the North Pacific, *Trans. AGU, 66*(51), 1326, 1986.

Feely, R. A., R. H. Byrne, J. G. Acker, P. R. Betzer, C.-T. A. Chen, J. F. Gendron, and M. F. Lamb, Winter-summer variations of calcite and aragonite saturation in the northeast Pacific, *Mar. Chem., 25,* 227–241, 1988.

Feely, R. A., M. F. Lamb, D. J. Greeley, and R. Wanninkhof, Comparison of the carbon system parameters at the global CO_2 survey crossover locations in the North and South Pacific Ocean, 1990–1996. ORNL/CDIAC-115, Carbon Dioxide Information Analysis Center, Oak Ridge National Laboratory, U.S. Department of Energy, Oak Ridge, Tenn., 74 pp., 1999.

Fiadeiro, M., The alkalinity of the deep Pacific, *Earth Planet. Sci. Lett., 49*, 499–505, 1980.

Gruber, N., J. L. Sarmiento, and T. F. Stocker, An improved method for detecting anthropogenic CO_2 in the oceans, *Global Biogeochem. Cycles, 10*, 809–837, 1996.

Harris, R. P., Zooplankton grazing on the coccolithophore Emiliani huxleyi and its role in the inorganic carbon flux, *Mar. Biol., 119*, 431–439, 1994.

Honjo, S., Biogenic carbonate particles in the ocean; Do they dissolve in the water column?, in *The Fate of Fossil fuel CO_2 in the Oceans*, edited by N. R. Anderson and A. Malahoff, pp. 269–294, Plenum Pub, New York, 1977.

Honjo, S., J. Dymond, R. Collier, and S. J. Manganini, Export production of particles to the interior of the equatorial Pacific Ocean during the 1992 EqPac experiment, *Deep-Sea Res. II, 42*, 831–870, 1995.

Jansen, H., and D. A. Wolf-Gladrow, Carbonate dissolution in copepod guts: a numerical model, *Mar. Ecol. Prog. Ser., 221,* 197–207, 2001.

Kanamori, S., and H. Ikegami, Calcium-alkalinity relationship in the North Pacific, *J. Oceanogr. Soc. Japan, 38,* 57–62, 1982.

Kleypas, J. A., R. W. Buddemeier, D. Archer, J.-P. Gattuso, C. Langdon, and B. N. Opdyke, Geochemical consequences of increased atmospheric carbon dioxide on coral reefs, *Science, 284,* 118–120, 1999.

Lamb, M. F., C. L. Sabine, R. A. Feely, R. Wanninkhof, R. M. Key, G. C. Johnson, F. J. Millero, K. Lee, T.-H. Peng, A. Kozyr, J. L. Bullister, D. Greeley, R. H. Byrne, D. W. Chipman, A. G. Dickson, C. Goyet, P. R. Guenther, M. Ishii, K. M. Johnson, C. D. Keeling, T. Ono, K. Shitashima, B. Tilbrook, T. Takahashi, D. W. R. Wallace, Y. Watanabe, C. Winn, and C. S. Wong, Consistency and synthesis of Pacific Ocean CO_2 survey data, *Deep-Sea Res. II, 49,* 21–58, 2002.

Lee, K., Global net community production estimated from the annual cycle of surface water total dissolved inorganic carbon, *Limnol. Oceanogr., 46*(4), 1287–1297, 2001.

Lewis, E., and D. W. R. Wallace, Program developed for CO_2 system calculations, Report 105, Oak Ridge National Laboratory, 33 pp., 1998 (also available currently at: http://cdiac.esd.ornl.gov/oceans/co2rprt.html).

Li, Y. H., T. Takahashi, and W. S. Broecker, Degree of saturation of $CaCO_3$ in the oceans, *J. Geophys. Res., 74,* 5507–5525, 1969.

Merhbach, C., C. H. Culberson, J. E. Hawley, and R. M. Pytkowicz, Measurement of the apparent dissociation constants of carbonic acid in seawater at atmospheric pressure, *Limnol. Oceanogr., 18*, 897–907, 1973.

Millero, F. J., Thermodynamics of the carbon dioxide system in the oceans, *Geochim. Cosmochim. Acta, 59*(4), 661–677, 1995.

Milliman, J. D., Production and accumulation of calcium carbonate in the ocean: Budget of a nonsteady state, *Global Biogeochem. Cycles, 7*, 927–957, 1993.

Milliman, J. D., and A. W. Droxler, Neritic and pelagic carbonate sedimentation in the marine environment: ignorance is not bliss, *Geol. Rundsch., 85*, 496–504, 1996.

Milliman, J. D., P. J. Troy, W. M. Balch, A. K. Adams, Y.-H. Li, and F. T. Mackenzie, Biologically mediated dissolution of calcium carbonate above the chemical lysocline, *Deep-Sea Res. I, 46*, 1653–1669, 1999.

Morse J. W., and F. T. Mackenzie, *Geochemistry of Sedimentary Carbonates,* Elsevier, New York, 707 pp., 1990.

Mucci, A., The solubility of calcite and aragonite in seawater at various salinities, temperatures and 1 atmosphere total pressure, *Am. J. Sci., 238*, 780–799, 1983.

Pond, D. W., R. P. Harris, and C. A. Brownlee, Microinjection technique using a pH sensitive dye to determine the gut pH of Calanus helgolandicus, *Mar. Biol., 123*, 75–79, 1995.

Rodier, M., and R. LeBorgne, Export flux of particles at the equator in the western and central Pacific Ocean, *Deep-Sea Res., 44,* 2085–2113, 1997.

Sabine, C. L., F. T. Mackensie, C. Winn, and D. M. Karl, Geochemistry of carbon dioxide in seawater at the Hawaii ocean time series station, ALOHA, *Global Biogeochem. Cycles, 9*(4), 637–651, 1995.

Sabine, C. L., R. M. Key, K. M. Johnson, F. J. Millero, A. Poisson, J. L. Sarmiento, D. W. R. Wallace, and C. D. Winn, Anthropogenic CO_2 inventory of the Indian Ocean, *Global Biogeochem. Cycles, 13*, 179–198, 1999.

Sabine, C. L., and R. A. Feely, Comparison of recent Indian Ocean anthropogenic CO_2 estimates with a historical approach, *Global Biogeochem. Cycles, 15*(1), 31–42, 2001.

Sabine, C. L., R. A. Feely, R. M. Key, J. L. Bullister, F. J. Millero, K. Lee, T.-H. Peng, B. Tilbrook, T. Ono, and C. S. Wong, Distribution of anthropogenic CO_2 in the Pacific Ocean, *Global Biogeochem. Cycles,* in press, 2002.

Stuiver, M., P. D. Quay, and H. G. Ostlund, Abyssal water carbon-14 distribution and the age of the world oceans, *Science, 219*, 849–851, 1983.

Sverdrup, H. U., N. W. Johnson, and R. H. Fleming, *The Oceans,* Prentice-Hall, Englewood, 1941.

Takahashi, T., Carbonate chemistry of seawater and the calcite compensation depth in the oceans, special publication of the Cushman Foundation, *Foraminiferal Res., 13,* 11–126, 1975.

Tsunogai, S., An estimate of the rate of decomposition of organic matter in the deep water of the Pacific Ocean, in *Biological Oceanography of the North Pacific Ocean*, edited by Y. Takenouti, pp. 517–533, Idemitsu, Shoten, Tokyo, 1972.

Tsunogai, S., H. Yamahata, S. Kudo, and O. Saito, Calcium in the Pacific Ocean, *Deep-Sea Res., 20*, 717–726, 1973.

Tsunogai, S., Application of a settling model to the vertical transport of soluble elements in the ocean, *Geochem. J., 12*, 81–88, 1978.

Tsunogai, S., and Y. Watanabe, Calcium in the North Pacific water and the effect of organic matter on the calcium-alkalinity relation, *Geochem. J., 15*, 95–107, 1981.

Tsunogai, S., and S. Noriki, Particulate fluxes of carbonate and organic carbon in the ocean. Is the marine biological activity working as a sink of atmospheric carbon? *Tellus, 43B*, 256–266, 1991.

Van der Wal, P., R. S. Kempers, and M. J. W. Veldhuis, Production and downward flux of organic matter and calcite in a North Sea bloom of the coccolithophore *Emiliania huxleyi*, *Mar. Ecol. Prog. Ser., 126*, 247–265, 1995.

Warner, M. J., J. L. Bullister, D. P. Wisegarver, R. H. Gammon, and R. F. Weiss, Basin-wide distributions of chlorofluorocarbons CFC-11 and CFC-12 in the North Pacific: 1985–1989, *J. Geophys. Res., 101*(C9), 20,525–20,542, 1996.

R. A. Feely, M. F. Lamb, D. Greeley, J. L. Bullister, NOAA/PMEL, 7600 Sand Point Way NE, Seattle, WA 98115-6349, USA. (feely@pmel.noaa.gov)

C. L. Sabine, Joint Institute for the Study of Atmosphere and Ocean, University of Washington, c/o NOAA/PMEL, 7600 Sand Point Way NE, Seattle, WA 98115, USA.

K. Lee, School of Environmental Science and Engineering, Pohang University of Science and Technology, San 31, Nam-gu, Hyoja-dong, Pohang, Republic of Korea.

F. J. Millero, University of Miami/RSMAS, 4600 Rickenbacker Causeway, Miami, FL 33149, USA.

R. M. Key, AOS Program, Princeton University, Forrestal Campus/Sayre Hall, Princeton, NJ 08544, USA.

T. -H. Peng, NOAA/Atlantic Oceanographic and Meteorological Laboratory, 4301 Rickenbacker Causeway, Miami, FL 33149, USA.

A. Kozyr, Carbon Dioxide Information Analysis Center, ORNL, Oak Ridge, TN 37831, USA.

T. Ono, Hokkaido National Fisheries Research Institute, 116 Katsurakoi, Kushiro 085-0802, Japan.

C. S. Wong, Institute of Ocean Sciences, 9860 W. Saanich Road, Sidney, British Columbia V8L 4B2, Canada.

(Received _____.)

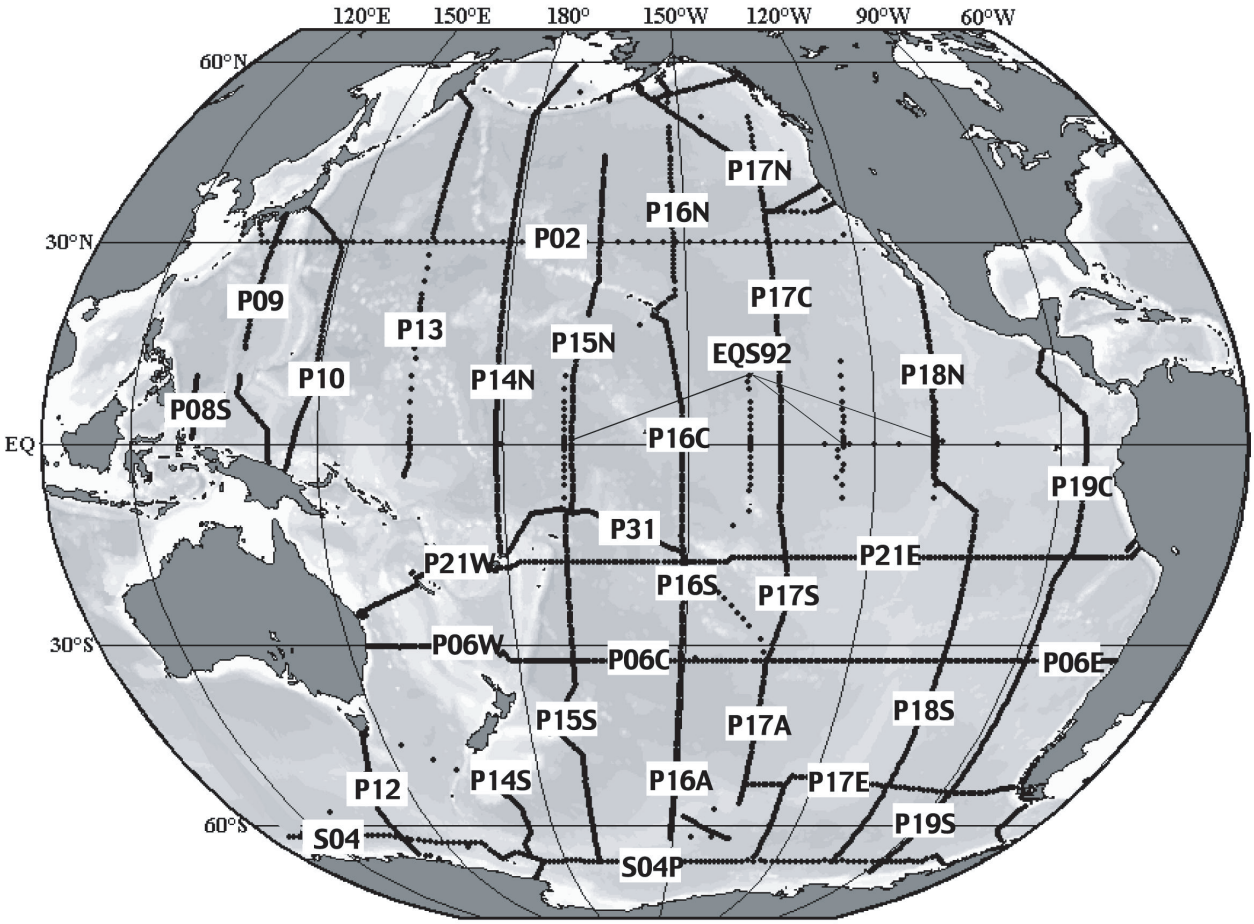

Figure 1. Map of the station locations for the international WOCE/JGOFS global CO_2 survey in the Pacific Ocean (1991–1996).

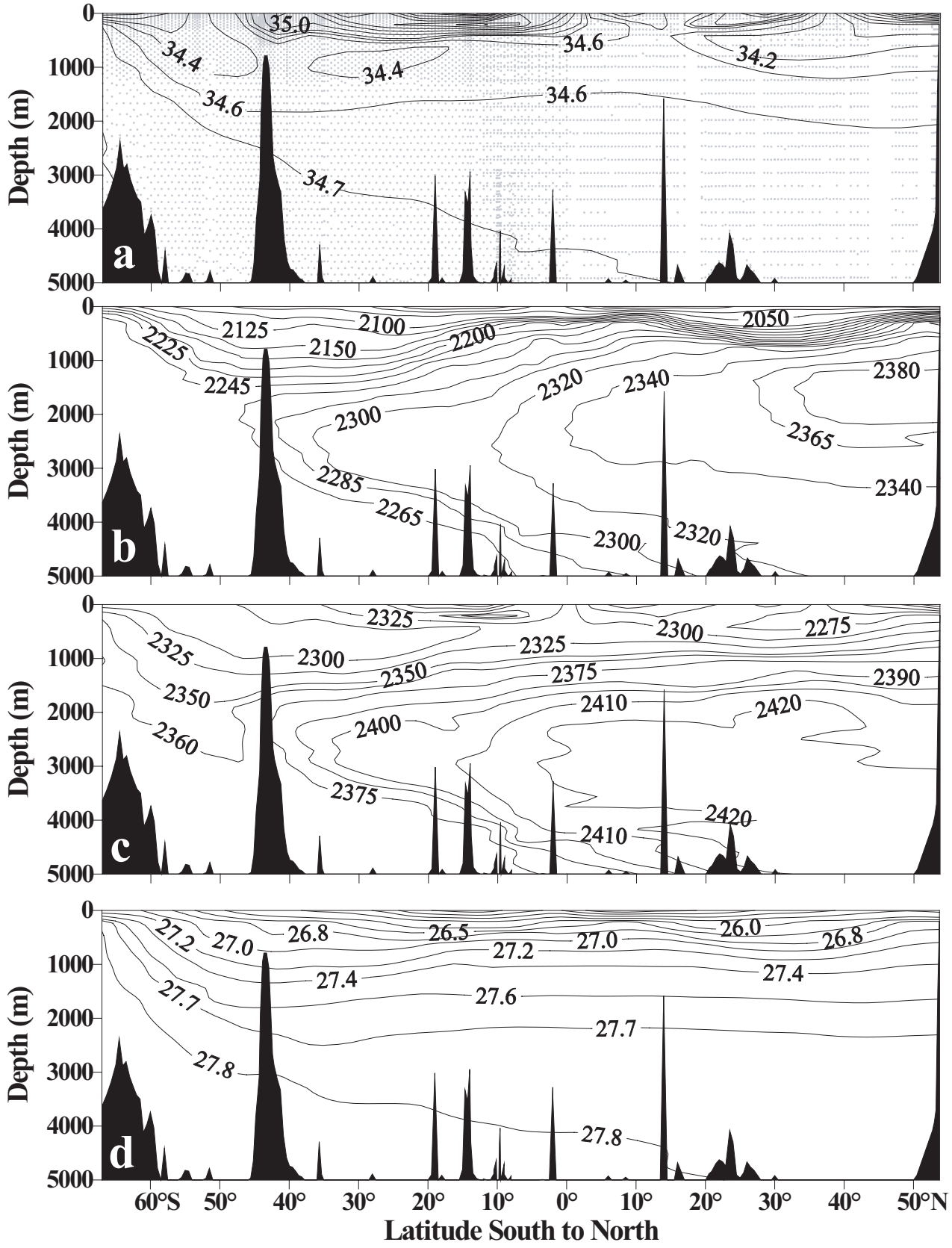

Figure 2. Vertical distributions of (a) salinity, (b) DIC in μmol kg^{-1}, (c) TA in μmol kg^{-1}, and (d) potential density, σ_θ, in the WOCE/JGOFS section P15S and P15N along 170°W in the Pacific.

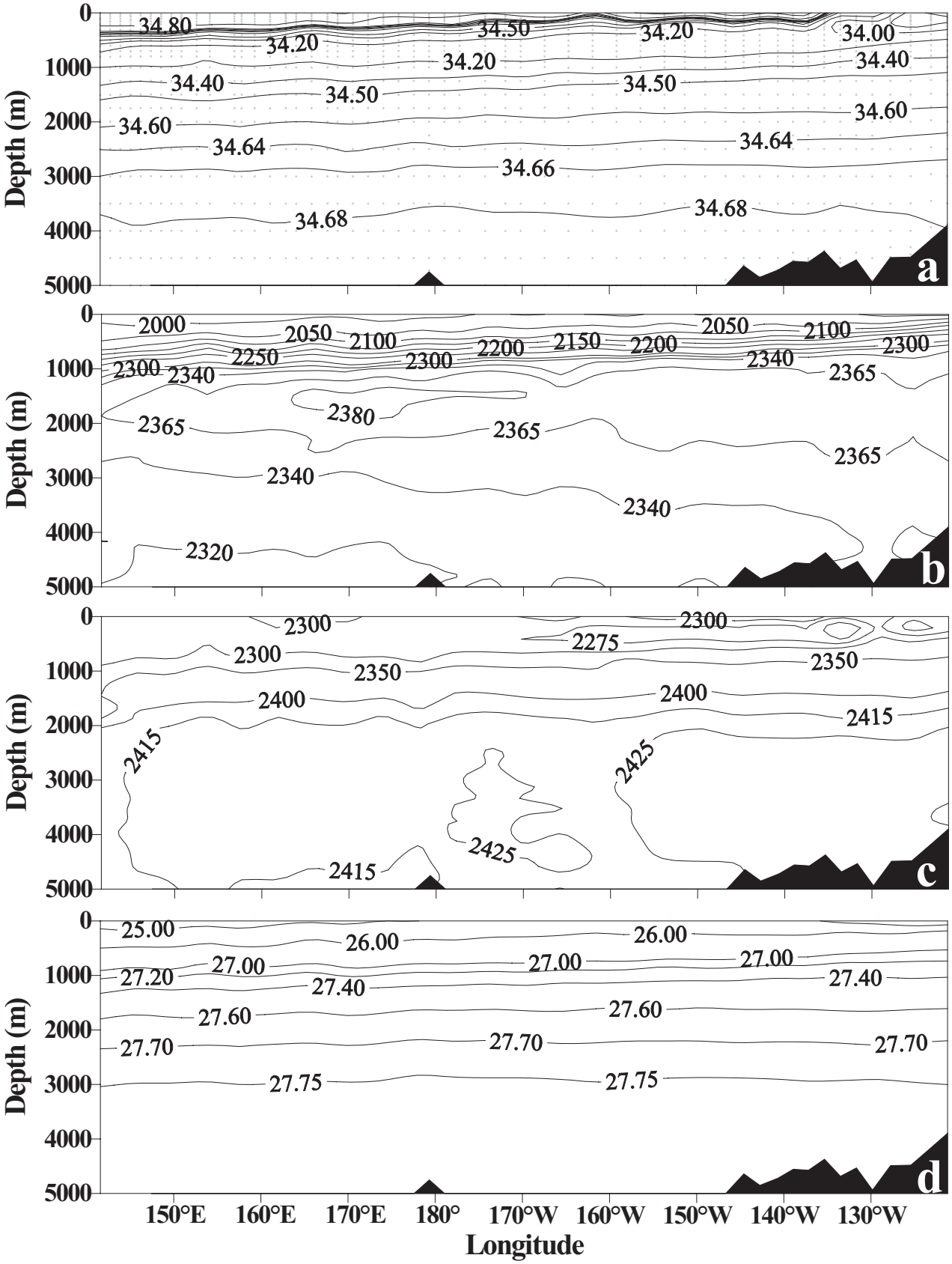

Figure 3. Vertical distributions of (a) salinity, (b) DIC in μmol kg^{-1}, (c) TA in μmol kg^{-1}, and (d) potential density, σ_θ, in the WOCE/JGOFS section P2 along 30°N in the North Pacific.

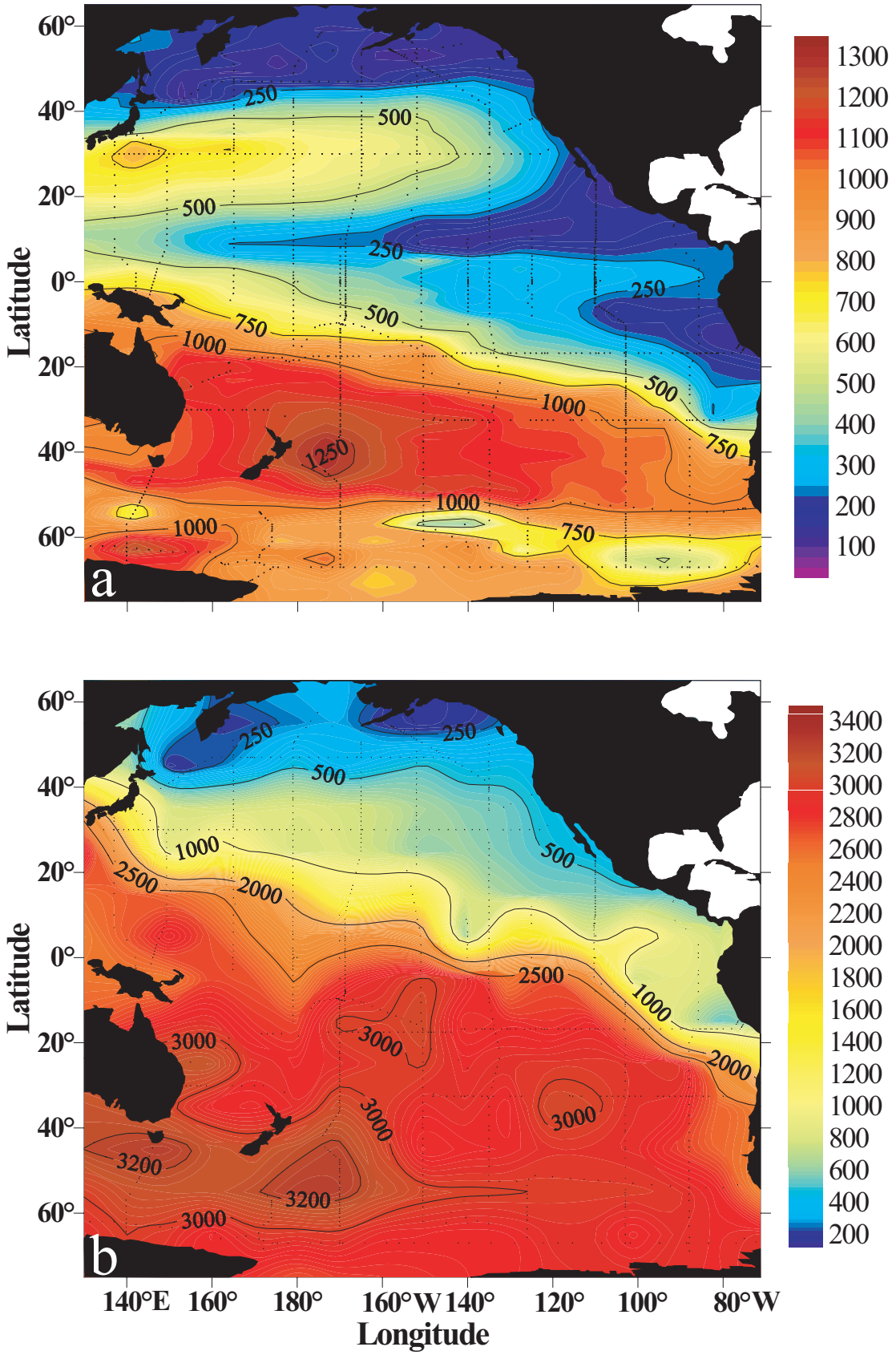

Figure 4. Saturation depth in meters for (a) aragonite and (b) calcite estimated from water column DIC and TA concentrations.

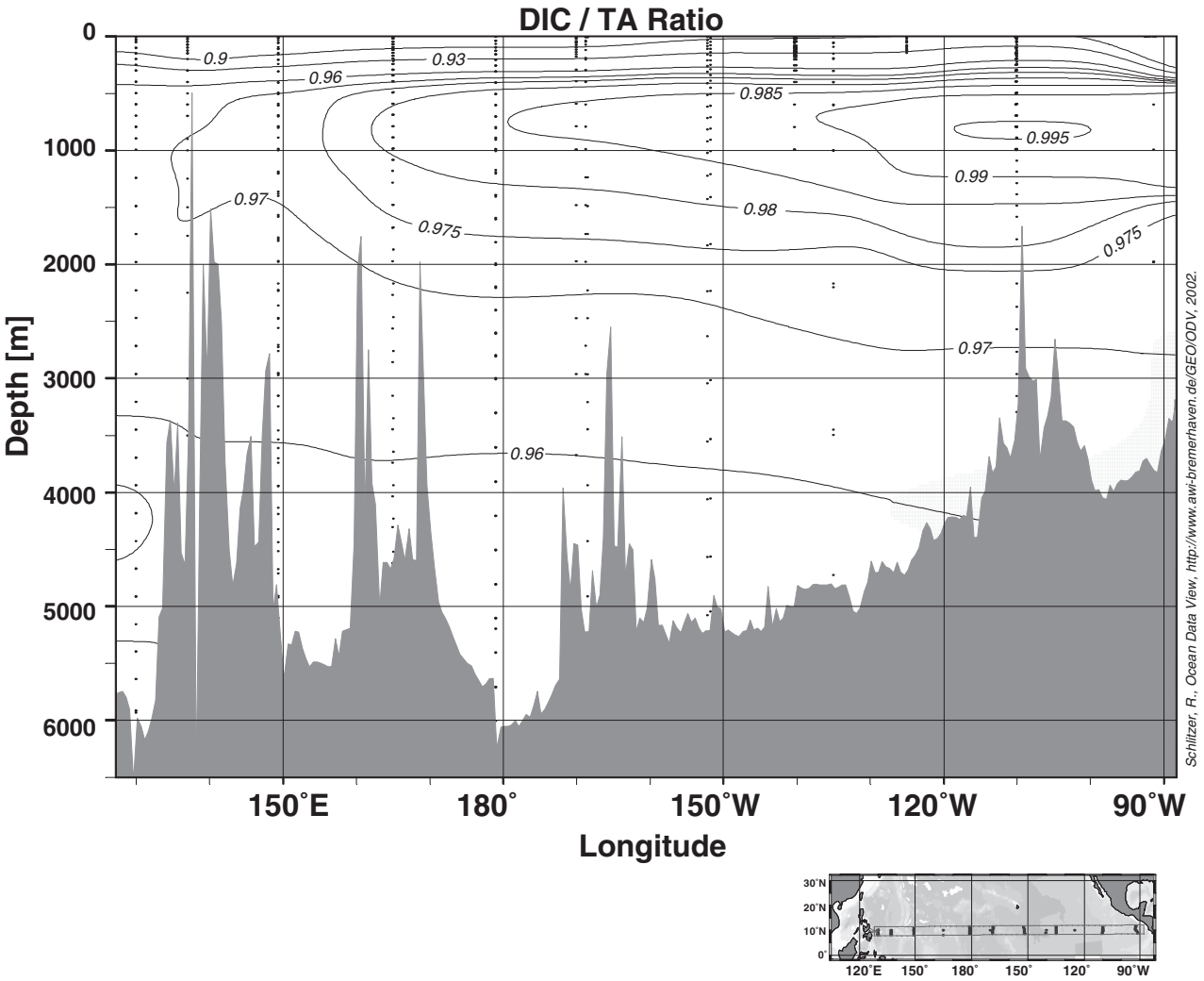

Figure 5. East-west section of DIC/TA ratio along 30°N in the North Pacific.

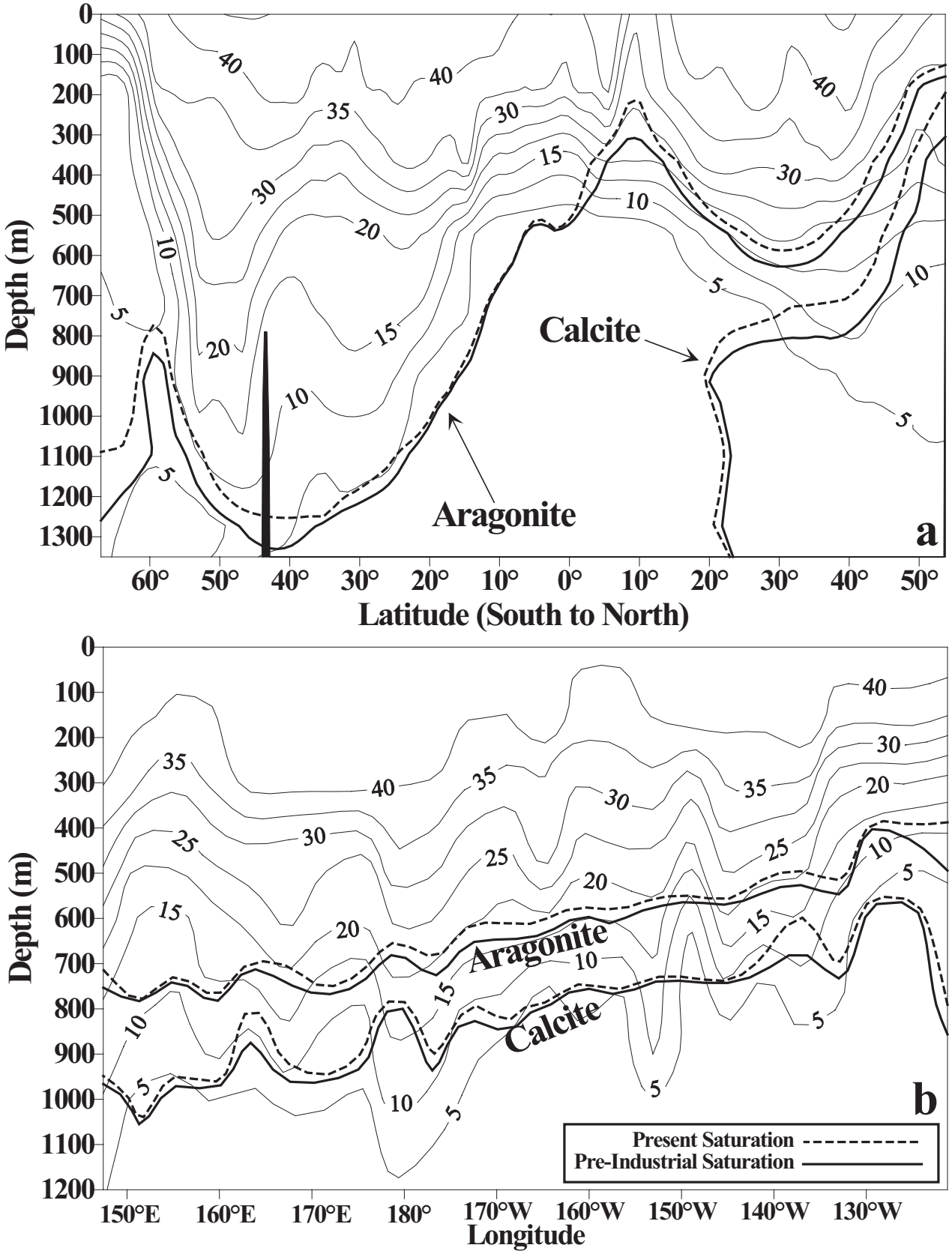

Figure 6. Vertical distributions of anthropogenic CO_2 concentrations in μmol kg^{-1} and the supersaturation/undersaturation horizons for aragonite and calcite along (a) WOCE/JGOFS section P15S and P15N, and (b) WOCE/JGOFS section P2 in the Pacific Ocean.

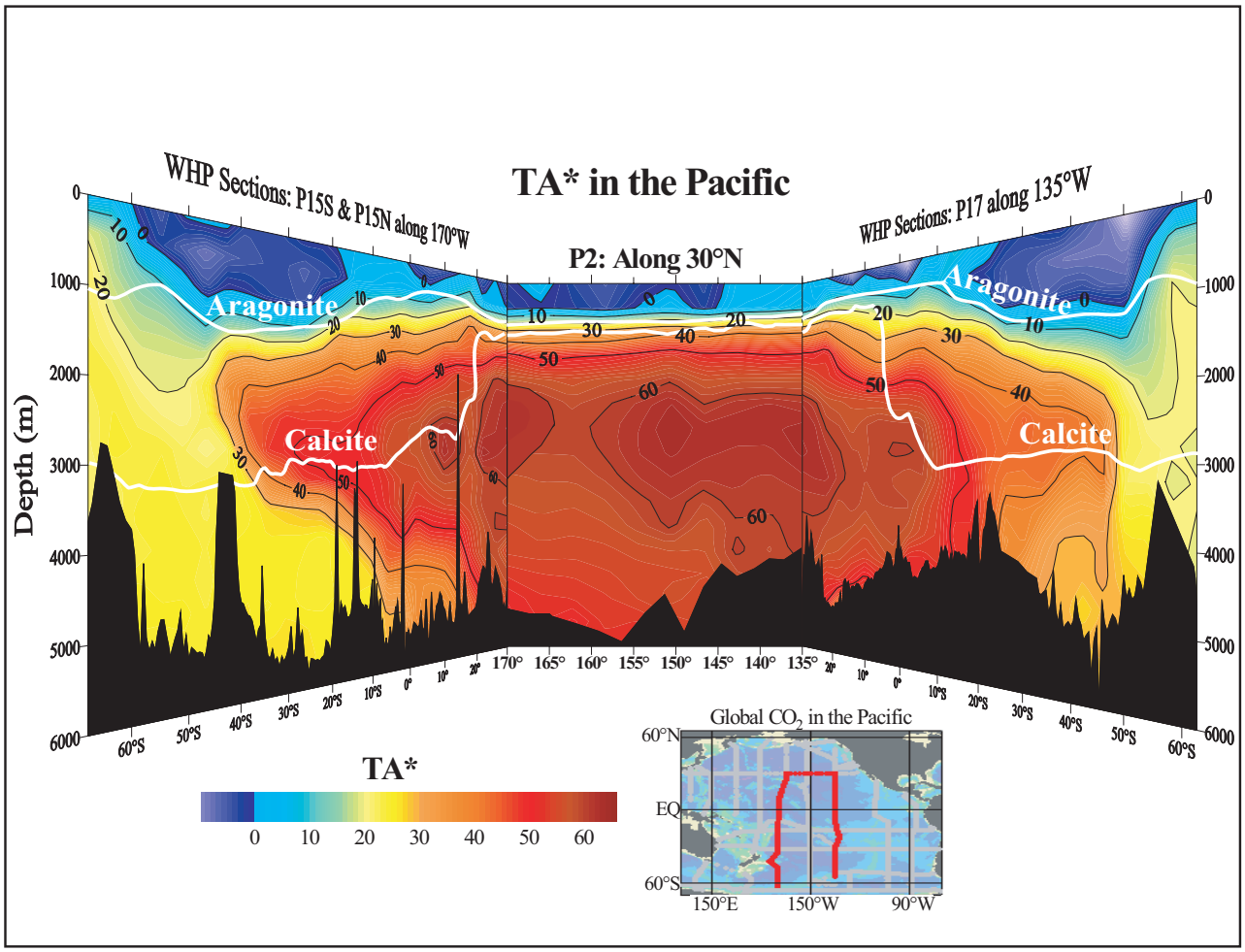

Figure 7. Wedge-like cutout section of TA* in μmol kg^{-1} along 170°W, 30°N, and 135°W in the Pacific Ocean.

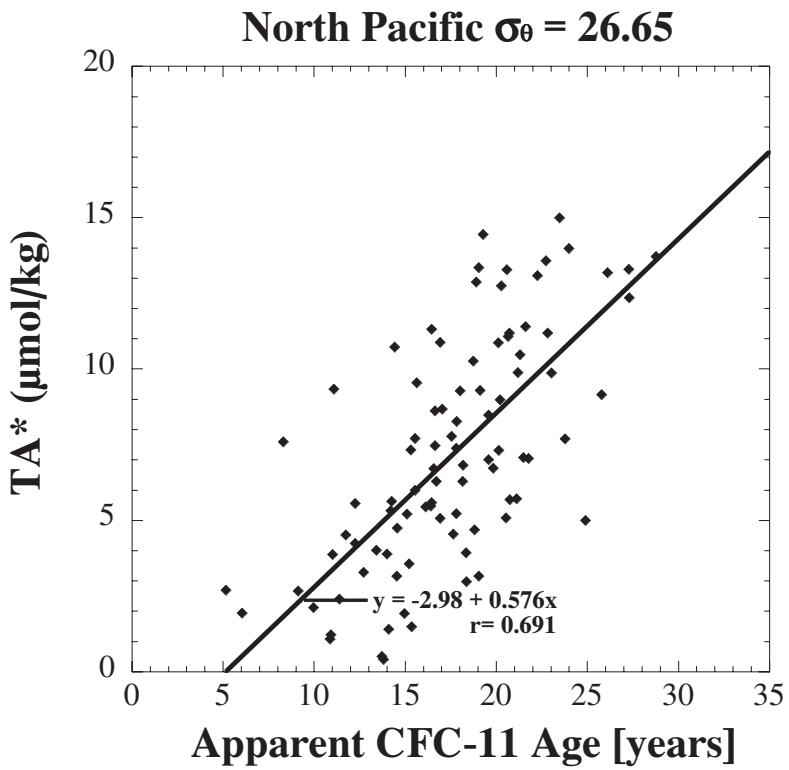

Figure 8. Plot of TA* versus CFC-11 age for data collected along the 26.65 σ_θ surface in the North Pacific Intermediate Water.

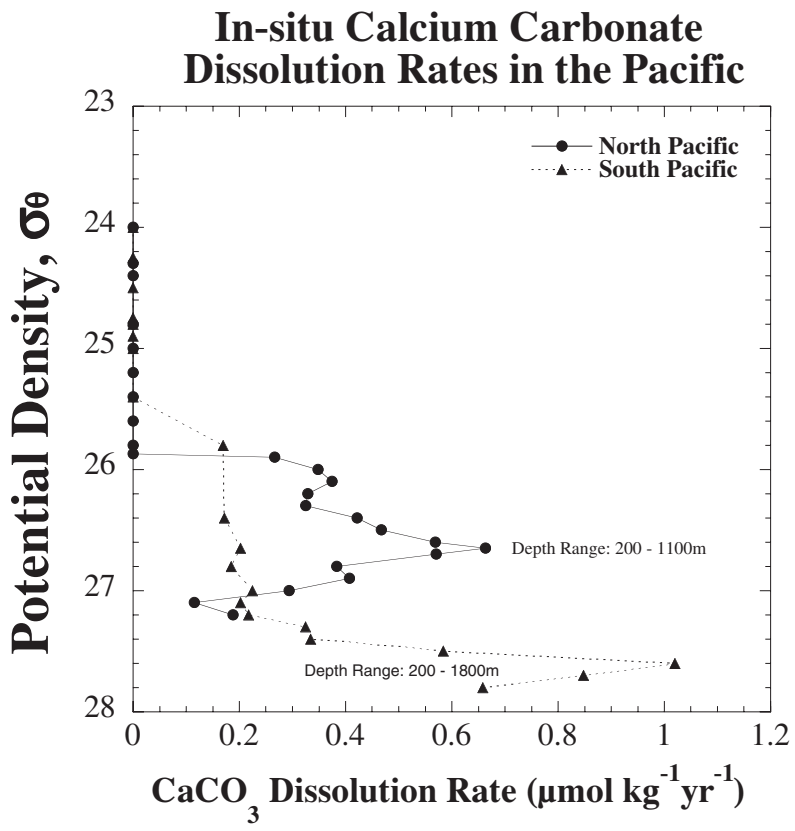

Figure 9. In situ calcium carbon dissolution rates plotted as a function of potential density in the Pacific Ocean.

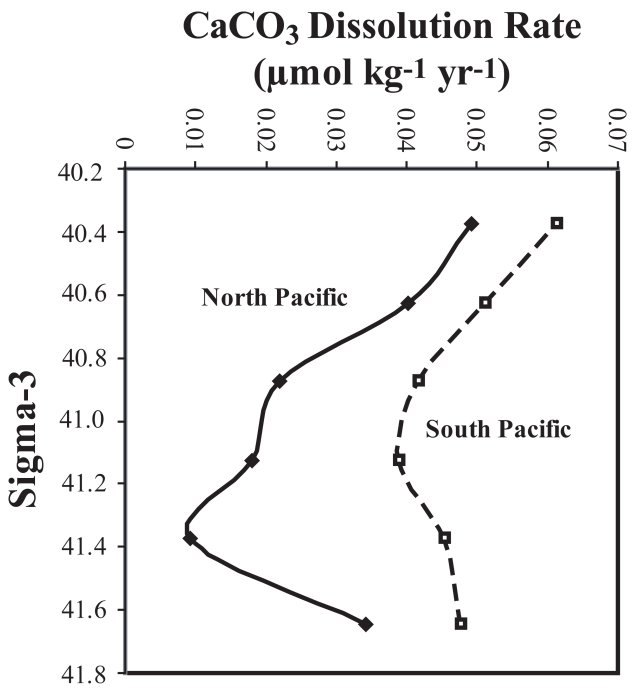

Figure 10. Vertical profiles of average deepwater $CaCO_3$ dissolution rates in the North and South Pacific plotted as a function of σ_3.

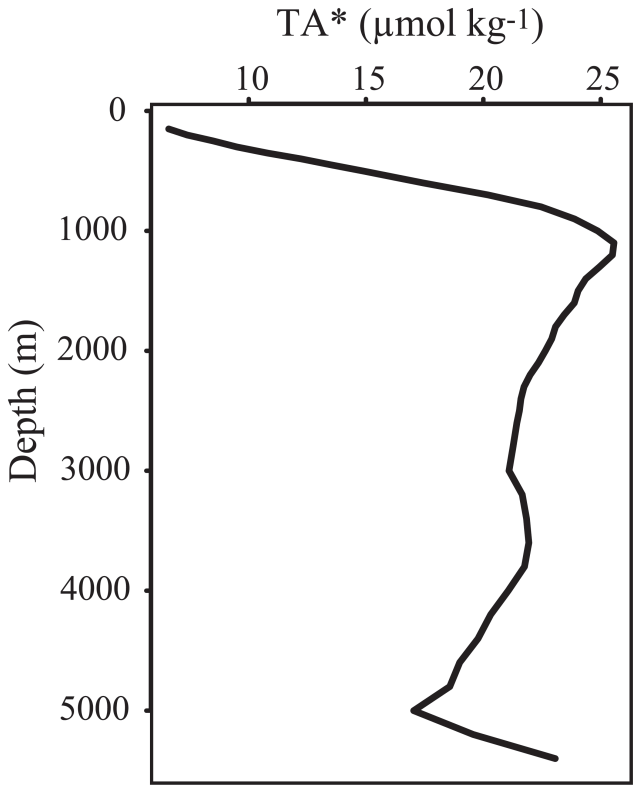

Figure 11. Plot of the average vertical profile of TA^* in units of μmol kg^{-1} for the Pacific Ocean.

Table 1. In Situ Calcium Carbonate Dissolution Rates in the Pacific Ocean

Study Reference	Depth Range (km)	$CaCO_3$ Dissolution Rate (μmol kg^{-1} yr^{-1})
Deep Water Column		
Li et al. [1969]	>1	0.09
Tsunogai [1972]	>1	0.048
Tsunogai et al. [1973]	<4	0.04 and 0.11
Edmond [1974]	<5	0.048
Fiadeiro [1980]	>1	0.06
Tsunogai and Watanabe [1981]	>1	0.057
Feely et al. [1986] (TA and Ca data)	>1	0.06
Chen [1983, 1990]	>2	0.072
Chen [1983] (TA data)	>2	0.053
Chen [1983] (Ca data)	>2	0.06
This Study (TA data)	>1.0	0.051
Deep Sediment Trap Studies		
Tsunogai and Noriki [1991]	0.5–1	0.02
	1–2	0
	2–3	0.006
	3–4	0.003
	4–5	0
Equatorial Pacific [Honjo et al., 1995]		
5°N	2.2–3.9	0.014
EQ	2.3–3.6	0.008
12°S	1.3–3.6	0.005
Shallow Water Dissolution		
Honjo et al. [1995] Traps (spring)	0.1–1	1.83
Betzer et al. [1984]	0.1–1	0.12
Rodier and LeBorgne [1997] Floating traps	0.1–0.32	0.68
Milliman et al. [1999]	0.35–0.5	1.56
This Study (TA data)	0.2–1.1	0.36